The Synthesis and Characterization of
$[Er(pzdo)_2(H_2O)_4](CF_3SO_3^-)_3 \bullet 3(H_2O) \bullet 1/2(pzdo)$



James Dennis Buchner Jr.

Department of Chemistry
Allegheny College
Meadville, PA 16335

Submitted: April 6, 2009

The Synthesis and Characterization of
$[Er(pzdo)_2(H_2O)_4](CF_3SO_3^-)_3 \bullet 3(H_2O) \bullet 1/2(pzdo)$

James Dennis Buchner Jr.

A Senior Comprehensive Project
Department of Chemistry
Allegheny College

Submitted to the Allegheny College Department of Chemistry in partial fulfillment of the requirements for the degree of Bachelor of Science

Senior Project Committee Members:

Dr. Jacqueline Knaust
Dr. P.J. Persichini III
Dr. Vladi Heredia-Wilent

Date: April 6, 2009

I hereby recognize and pledge to fulfill my responsibilities, as defined by the Honor Code, and to maintain the integrity of both myself and the college community as a whole.

Pledge: _____

Word Count: 8.254

Acknowledgments
(II)

To My Parents: Without your guidance and support there is no way that I would have ever made it this far in Chemistry and in life. Through everything you both never lost faith in me and were there anytime I was in need. You are both the most generous and caring people in the world and I can only hope to emulate your hard work and determination in my life. I love you both more than words can describe.

To Dr. Knaust: Well, my path towards a degree in Chemistry started with your 110 class three years ago, and you have been there for me every day since. I know I haven't always been the easiest advisee, but what can I say, I like to make things interesting. I can't thank you enough for you help on the crystal structures and all of the data interpretation, without your help I would have never been able to put this paper together.

To the Chemistry Department: Thank you to all of the professors who I have had the privilege of studying under. You all have made this a wonderful journey; I will remember each of you forever.

To Drs. Persichini and Wilent: Thank you for your guidance through this entire senior project process. Your feedback has made me push myself to learn more about lanthanide networks, and also taught me how to put my best foot forward when presenting to an audience. Also, thank you both so much for you assistance on the letters of recommendation. I know your schedules are long and demanding and I really appreciate the time you took to sit down and do that favor for me.

To The Brothers of Sigma Alpha Epsilon: Well, our time together is finally drawing to a close. While I know I will be back and see each of you very soon, I wish nothing but good things for all of you. Each of you has had a large impact on my college career, and most definitely you have helped me come a little bit closer to becoming a True Gentleman.

To Dr. Zeller and YSU: Thank you so much for helping me attempt to understand how to run the X-Ray defractometer. Your help in the scanning and refinement process has been invaluable to me all these years.

To Evanee: I am so happy to have met you that one day in Schultz. While I never would have guessed that things would have turned out this way, I definitely could not be any happier. Having you and Havisham around made my time at Allegheny so much better, I love you.

TABLE OF CONTENTS
(III)

I) Pledge, Word Count and Information…… 2

II) Acknowledgments……. 3

III) Table of Contents …….. 4

IV) Abstract ……. 5

V) Introduction ……... 6

VI) Experimental

A) Synthesis of Pyrazine-N,N'-dioxide…… 19

B) Preparation of Erbium Triflate solution……. 20

C) Synthesis of the coordination polymer ……. 20

D) X-Ray Diffraction…….. 22

VII) Results and Discussion …… 24

VIII) Conclusions …… 35

IX) Data Analysis …… 37

X) Crystal Data and Appendix …… 39

XI) References …… 51

Abstract
(IV)

Coordination polymer compounds employ several types of intermolecular forces. Synthesis of these compounds requires consideration of ligand properties necessary to arrive at a final target with specific properties. Lewis acid and base attractions are necessary to bind the metal and bridging ligands that link each metal center to the next and form the network. The ligand pyrazine-N,N'-dioxide was synthesized and combined with various lanthanide triflate salts in an attempt to synthesize a novel coordination network. A reaction between $Er(CF_3SO_3)_3$ and pyrazine-N,N'-dioxide yielded the two-dimensional lanthanide coordination network; $[Er(pzdo)_2(H_2O)_4](CF_3SO_3^-)_3 \bullet 3(H_2O) \bullet 1/2(pzdo)$

Introduction
(V)

In recent years, there has been significant interest in the design of coordination compounds with tailored frameworks suitable for a wide variety of chemical applications. Catalytic, gas interaction, optical, electronic and magnetic properties can be tailored under the right chemical synthesis conditions.[i] Much of the research in this field has focused on the design and function of metal-organic-metal frameworks with d-block transition-metal ions.[ii,iii] These metal-organic compounds have been noted to form one-, two-, and three-dimensional frameworks depending on the chemical environment as well as constituent ligands bound to the metal center.[iv]

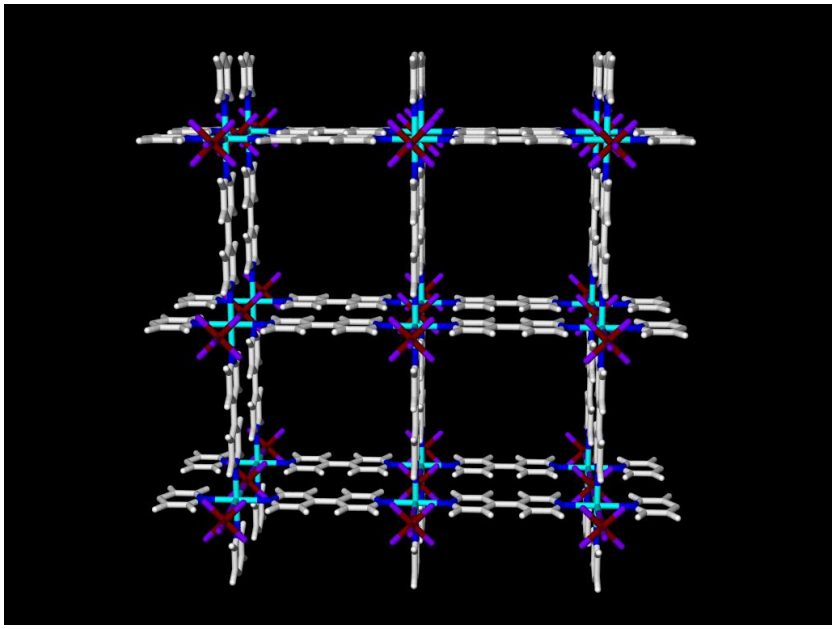

Figure 1:[v] Wire-frame representation of the 3-D network [Zn(4,4'-bipyridine)$_2$(SiF_6)$_2$]. The Si atoms are wine colored, Zn metal centers are aqua colored, hydrogen atoms have been omitted for clarity.

The frameworks can build upon one another through hydrogen bonding, π- π stacking, and other weak binding forces to form three-dimensional networks whose properties have been studied by many research groups.[vi] In the example shown in Figure 1, the Zn^{2+}

centers are further coordinated by the fluorine atoms of the of the SiF_6 counter ions in the axial positions that also act to crosslink the grids to form the pseudo-octahedral coordination polymer. Network formations such as this allow for a large number of coordination geometries and porous networks to be formed where individual characteristics can be studied.

Metal-organic-metal complexes have been studied extensively in the past using organic ligands and transition metal centers with coordination numbers ranging from two to six. Since these compounds have many potential applications, it is necessary to explore new building blocks and building principles to evaluate larger and more diverse coordination networks. Substitution of a lanthanide metal in place of a transition metal raises a number of challenges. Coordination diversity, high coordination numbers with flexible geometry, and the poor stereo-chemical preference of the lanthanide ions cause problems with unusual network configurations and topologies.[vii] On the other hand, since the lanthanide metals fill the 4f orbital, their atomic and ionic radii are significantly larger than those of the transition metals. Cu^{2+} and Zn^{2+}, for instance, have ionic radii of 0.72 A and 0.74 A respectively; whereas, the lanthanide series ionic radii vary from La^{+3} at 1.07 A, to Lu^{+3} at 0.85 A.[viii] The reduction of radius with increasing 4f shell fill is referred to as 'lanthanide contraction' and is a result of the increasing nuclear charge overcoming the increased 4f shell electron population. In any case, and especially with the lower atomic number lanthanides, the increase in ionic radii permits the use of more and larger ligands. Coordination numbers of up to 12 are possible with lanthanide metal coordinate compounds.[ix] Consideration of what properties are preferred in a ligand should be given when constructing any type of metal-organic-metal coordination network.

Synthesis of coordination compounds involves the formation of coordinate covalent bonds (formerly referred to as dative bonds) between an 'electron deficient' metal ion and an 'electron rich' electron donor called a ligand. The concept of Lewis acid and Lewis base describes the ability of the metal and ligand respectively to either accept or donate electrons in bond formation. In 1963, Pearson et al. attempted to describe Lewis acidity in terms of chemical "hardness" or "absolute electronegativity".[x] This concept measures the escaping tendency, or resistance to change electron density from a molecule or ion (any collection of nuclei and electrons). The original basis of the concept was put forth to explain why some metal ions form very stable complexes in solution with iodide ions and weak, or no complexes, with fluoride ions. Using the hard and soft acid and base (HSAB) principle it has been possible to summarize a great deal of diverse chemical information through categorization of ions or molecules as either hard or soft. Hard acids prefer to coordinate with hard bases whereas soft acids prefer to coordinate with soft bases. Soft-soft combinations result in a bond with higher covalent character while hard-hard combinations result in a bond with higher ionic character.

In 1983, Pearson and Parr extended the qualitative HSAB theory with a more quantitative expression of chemical hardness.[xi] The derived expression implies that the chemical hardness is proportional to the band gap in ionization potential and electron affinity. An operational definition is described in the following equation[xii]:

$$\text{Chemical Hardness} = \eta = \tfrac{1}{2}(I_s - A_s)$$

where I_s = ionization potential
A_s = electron affinity

For the lanthanide metals, the hardness parameter can be approximated as the difference in third and fourth ionization potentials (using erbium as the example):

A_s = Electron affinity $\cong Er^{+3} + e^- \rightarrow Er^{+2}$ = 22.74 eV

I_s = Ionization Potential $\cong Er^{+3} \rightarrow Er^{+4} + e^-$ = 42.7 eV

$\eta = \frac{1}{2}(I_s - A_s)$
$= \frac{1}{2}$ (42.7eV – 22.74 eV)
= 9.98 eV

Similar treatment for the entire lanthanide series produces the following table:

Chemical Hardness		**A_s**	**I_s**		**η**
Ionization Energy	**II**	**III**	**IV**	**IV-III**	**(IV-III)/2**
	ev	**ev**	**ev**	**ev**	**ev**
Lanthanide					
La	11.06	19.18	49.95	30.77	15.39
Ce	10.85	20.20	36.76	16.56	8.28
Pr	10.55	21.62	38.98	17.36	8.68
Nd	10.72	22.10	40.40	18.30	9.15
Pm	10.90	22.30	41.10	18.80	9.40
Sm	11.07	23.40	41.40	18.00	9.00
Eu	11.25	24.92	42.70	17.78	8.89
Gd	12.09	20.63	44.00	23.37	11.69
Tb	11.52	21.91	39.79	17.88	8.94
Dy	11.67	22.80	41.47	18.67	9.34
Ho	11.80	22.84	42.50	19.66	9.83
Er	11.93	22.74	42.70	19.96	9.98
Tm	12.05	23.68	42.70	19.02	9.51
Yb	12.18	25.05	43.60	18.55	9.28
Lu	13.90	20.96	42.25	21.29	10.65

Table 1: Calculated chemical hardness parameters for the lanthanide series metal +3 ions using the band gap of ionization potentials method. The second, third, and fourth ionization energies were obtained from the CRC 88th edition.[xiii] The final two rows (change from third to fourth IE, and half of this same change) were calculated from the CRC data.

Two tables are included from the 1983 paper of Pearson and Parr. Table 2 shows the chemical hardness parameters for a wide range of metal ion Lewis acids. The chemical hardness for La^{+3} as determined by Pearson & Parr is 15.4 eV, in excellent agreement with 15.39 eV using the band gap in ionization potential method described above.

Hardness Parameters, η_A, for Some Lewis Acids (eV)

Acid	I_A	A_A	η_A
Na^+	47.3	5.14	21.1
Rb^+	27.5	4.18	11.7
Cu^+	20.3	7.72	6.3
Ag^+	21.5	7.57	6.9
Au^+	20.5	9.22	5.7
Mg^{3+}	80.1	15.03	32.5
Ca^{2+}	51.2	11.87	19.7
Ti^{2+}	27.5	13.57	7.0
Mn^{2+}	33.7	15.14	9.3
Fe^{2+}	30.6	16.18	7.3
Ni^{2+}	35.2	18.15	8.5
Cu^{2+}	36.8	20.29	8.3
Zn^{2+}	39.7	17.96	10.8
Cd^{2+}	37.5	16.90	10.3
Hg^{2+}	34.2	18.75	7.7
Pb^{2+}	31.9	15.03	8.5
Ba^{2+}	35.5	10.00	12.8
Pd^{2+}	32.9	19.42	6.8
Al^{3+}	120.0	28.4	45.8
Sc^{3+}	73.9	24.8	24.6
Fe^{3+}	56.8	30.6	13.1
La^{3+}	**50.0**	**19.2**	**15.4**

Table 2[xiv]: chemical hardness data for an array of Lewis acids adapted from Pearson & Parr paper on Absolute Hardness

$$\eta_A = \frac{1}{2}\left(I_A - A_A\right)$$

The chemical hardness parameters for the lanthanides using this method are found to range from a maximum of 15.4 eV to a minimum of 8.3 eV. When compared with

other Lewis acid metal ions, the lanthanides must be considered borderline chemical hardness Lewis acids, on average similar with Fe^{+3}. A hard acid is generally one with high positive charge, small size, and having no easily polarized outer electrons while a soft acid is one with low positive charge, large size, containing polarizable outer electrons. It is logical that the lanthanides are of borderline chemical hardness since they are large ions with high positive charge, but the valence 4f electrons are highly shielded by 5s,d and 6s orbitals.

Table 3 depicts the chemical hardness for a number of common Lewis base ligands.

Hardness Parameters, η_B, for Some Lewis Bases (eV)

base	I_b	A_B	η_B
F^-	17.42	3.40	7.0
Cl^-	13.01	3.62	4.7
Br^-	11.84	3.36	4.2
I^-	10.45	3.06	3.7

H^-	13.59	0.75	6.8
CH_2^-	9.82	1.8	4.0
N_3^-	11.6	1.8	4.9
NH_2^-	11.3	0.74	5.3
OH^-	13.0	1.83	5.6
NO_2^-	12.9	3.99	4.5
CN^-	14.2	3.6	5.3
SH^-	10.4	2.3	4.1
ClO^-	11.1	2.2	4.5
CO	26	14.0	6.0
H_2O	26.6	12.6	7.0
H_2S	21	10.5	5.3
NH_3	24	10.2	6.9
PH_3	20	10	5.0

Table 3[xv]: chemical hardness data for an array of Lewis bases adapted from Pearson & Parr paper on Absolute Hardness

Inspection of Table 3 shows a much smaller range in the chemical hardness data for the bases, which to some extent is a limitation of the database. A base is generally considered soft when the donor atom is of low electronegativity, easily oxidized, highly polarizable, and has low energy empty orbitals. A hard base is one where the donor atom is highly electronegative, hard to oxidize, has low polarizability, and has only high energy empty orbitals.

With respect to general HSAB theory the borderline hardness lanthanide Lewis acids would have higher bonding preference for borderline hardness Lewis bases. Although not included in Table 3, pyridine is considered a borderline Lewis base due to its high polarizability. With regard to pyrazine-N,N'-dioxide (pzdo) (pyridine ring with two para nitrogens) the Table component, NO_2^-, also yields additional insight. This compound ($O = N \rightarrow O^-$) is close to a model for the N-oxide bond in pyrazine-N,N'-dioxide. The chemical hardness of NO_2^- is 4.5 eV, which is interpreted from the body of data as also borderline. Therefore, although direct chemical hardness data for pyrazine-

N,N'-dioxide is not available we conclude from available sub-structures that it is most likely a borderline Lewis base and therefore a good ligand candidate for Er^{+3} and other lanthanide +3 metal ions. HSAB theory does not preclude the formation of coordinate compounds from, for instance, a hard acid and a softer base, it does however describe a general preference and to a degree, bond strength and activation energy.

In practice, HSAB theory and the attendant quantitative estimates of chemical hardness serve only as guidelines. Complications such as the steric nature of the ligand or solvation can overshadow these HSAB approaches. In addition, other chemical structure preferences, such as having an aromatic ring in the ligand, may also prove useful when building coordination networks due to their ability to interact and layer via Π - Π stacking.[xvi] Hydrogen bonding may also be important and lead to the choice of a ligand that provides for extended hydrogen bonding outside the primary coordination sphere. Synthesis of pyrazine-N,N'-dioxide from its parent pyrazine creates a bridging ligand with charges on both of the N-oxide bound oxygens. The increased electron density on oxygen due to its negative charge increases the base hardness of the ligand over a C=O or N=O oxygen. The resulting coordinate covalent bond with the lanthanide metal is more ionic in nature. The pyrazine-N,N'-dioxide is bi-dentate and enables extensive bridging between adjacent metal centers.

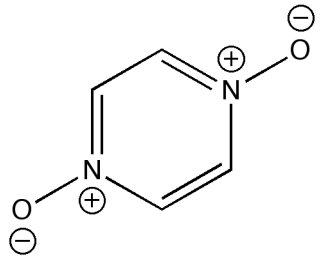

Figure 2: A ChemDraw® structure of pyrazine-N,N'-dioxide. The partial charges on both the oxygen and nitrogen atoms make this a very favorable bonding ligand for coordination networks.

Lanthanide coordination networks can yield greater flexibility to design custom frameworks for a variety of applications. Paz et al. designed and used X-Ray Diffraction (XRD) and solid-state NMR to characterize a number of lanthanide-organic networks for their high photoluminescence properties.[xvii] Figure 3 is a 3-D rendering of $[Pr(H_3NMP)]\cdot 1.5H_2O$ (nitrilotris(methylphosphonic acid) = (H_3NMP)).

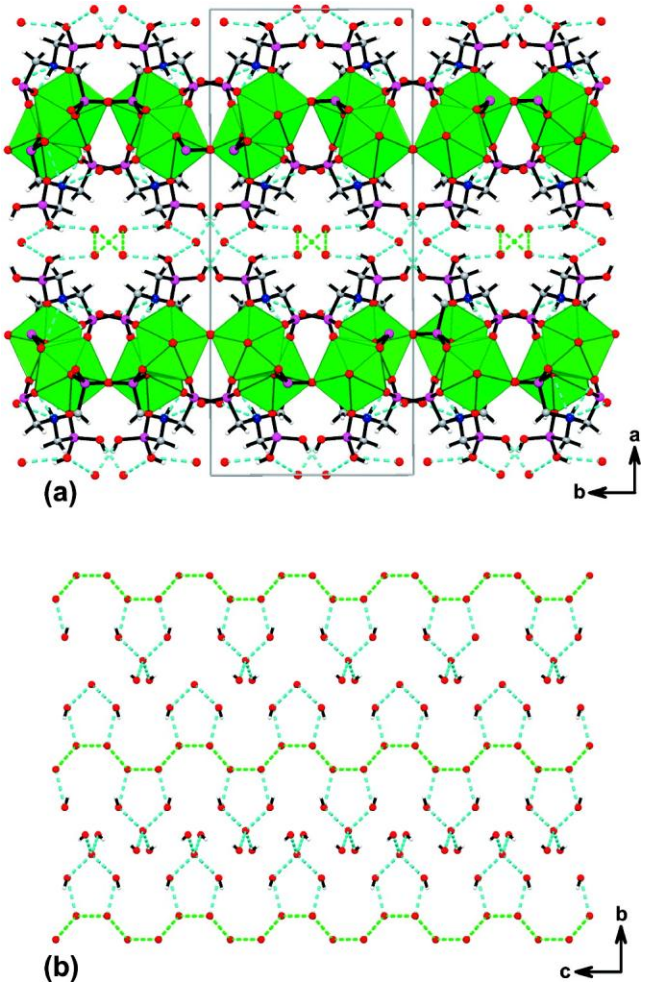

Figure 3:[xviii] (a) Crystal packing of $[Pr(H_3NMP)]\cdot 1.5H_2O$ viewed along the [001] direction of the unit cell. Hydrogen bonds are represented as dashed lines. (b) Hydrogen bonding sub-network involving the water molecules of crystallization.

Water to water interactions are represented as light green dashed bonds, while interactions between water and the [Pr(H_3NMP)] layers are drawn as light blue dashed lines.

While lanthanide coordination compounds have broad application potential, one of the most basic is that of catalysis in organic synthesis reactions. In heterogeneous catalysis, reactants are temporarily bound to a surface where bonds are strained in such a way as to lower the activation energy for their reaction. A number of laboratories have synthesized and evaluated various lanthanide coordination networks with organic ligands as catalysts for olefin and diene polymerization.[xix] Oliveira et al. used mono(cyclopentadienyl)lanthanide coordination compounds with pyrazinamide ligands as a catalyst for ethylene polymerization at 70ºC.[xx] Zocchi et al. synthesized $SmBr_3 \cdot 4iPr(OH)$, characterized the crystal structure, and evaluated it for polymerization activity using butadiene as a monomer at 50ºC.

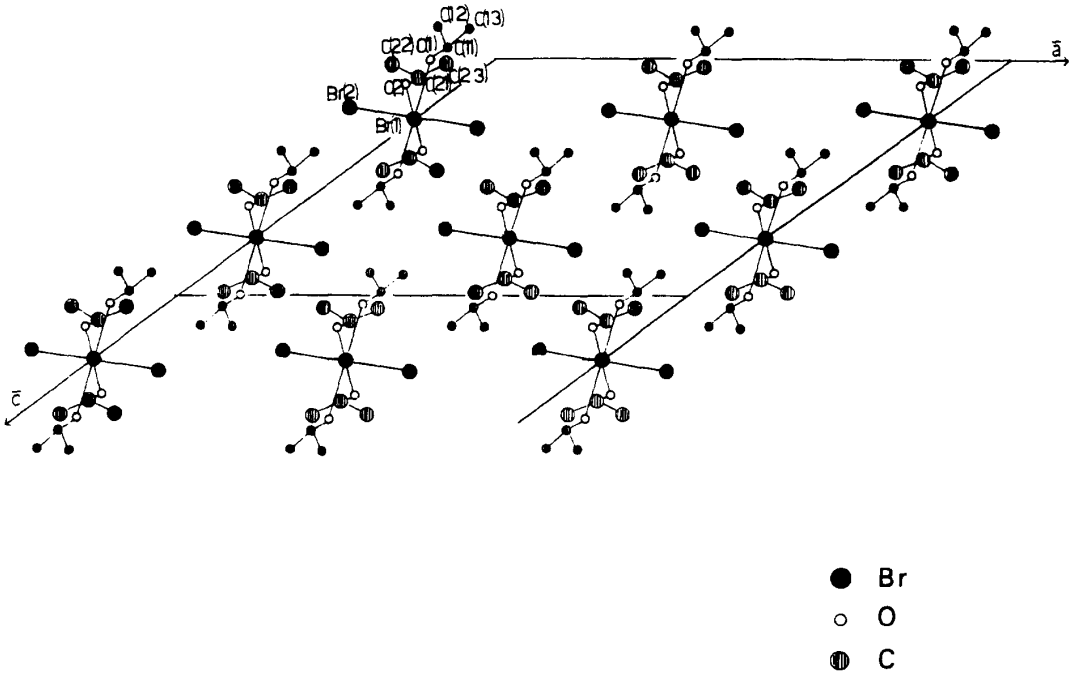

Figure 4:[xxi] A view of the proposed crystal structure along the b axis for $[SmBr_3(C_3H_7OH)_4]$. In the unit cell, the Sm is coordinated by 3 Br ions and by the oxygen atoms of the 4 isopropyl alcohol ligands. The Sm and Br(1) lie on the same axis of symmetry and therefore are superimposed in the figure.

It was found that the Sm^{+3} compounds exhibited a much lower catalytic activity than similar Nd^{+3} complexes.[xxii] The authors evaluated the diene polymerization activities of the systems prepared in their laboratory and also compared these data with those obtained in other laboratories including Hu et al.[xxiii] and Mikheen et al. whose summary is shown in Figure 5(b). Figure 5(a) plots the $E^0{}_{M^{3+}/M^{2+}}$ versus atomic number for the lanthanide series and Figure 5(b) plots the catalytic activity for the series with common ligand coordination.

The two plots show qualitative agreement indicating that the oxidation capacity of the lanthanide is an important factor in determining the catalytic activity.

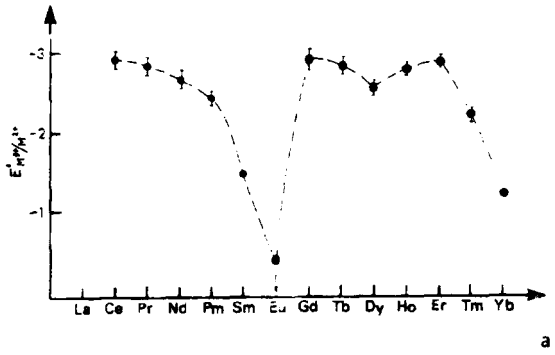

Figure 5:[xxiv] (a) Plot of $E^0_{M^{3+}/M^{2+}}$ observed for lanthanides as a function of their atomic number. (b) Conversion (%) from monomer to polymer of catalyst system based on Ln(naph), as a function of atomic number.

Prior Research

Prior research focused on the self-assembly of lanthanide coordination networks with early series lanthanide metals. La^{+3} (R = 1.14 A), Ce^{+3} (R = 1.07 A), and Pr^{+3} (R = 1.06 A) have been used to date. The primary ligand used was pyrazine N,N'-dioxide (pzdo). This ligand donor group coordinates to the lanthanide metal ion in the first coordination sphere through the oxygen atom. Since the pyridinium-N-oxide oxygen is highly electronegative and bound to the ring nitrogen that additionally bears a positive charge, the electron distribution creates a more polarized coordinate bond. This is essential to building the rigid frameworks that compose these coordination networks. This charge separation also potentially creates a unique condition to strain bonds in guest molecules (catalysis), or to adsorb or sequester gas molecules within the porous structure.

Based on preliminary XRD data obtained to date, the structures in Figures 6a and b are suggested for the $[La_2(pzdo)_6(CF_3SO_3)_2(H_2O)_6](CF_3SO_3^-)_4 \bullet (H_2O) \bullet 2(pzdo)$ synthesis previously described.

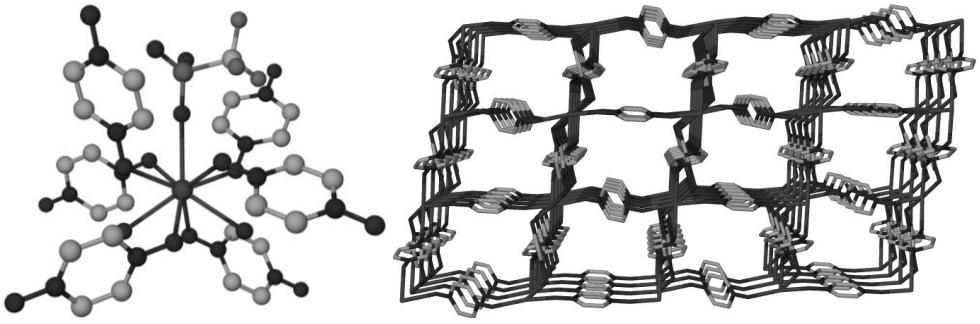

(a) (b)

Figure 6a: The coordination geometry of a single Lanthanum center coordinated to six pyrazine-N,N'-dioxide ligands, three water molecules, and a triflate group.
Figure 6b: A network of interconnected Lanthanum metal centers forming a 3-D sheet system, waters are omitted to reveal the porous network structure.

A layering method was used for the praseodymium coordination network and produced data which suggested the structure assignments in Figures 7a and b.

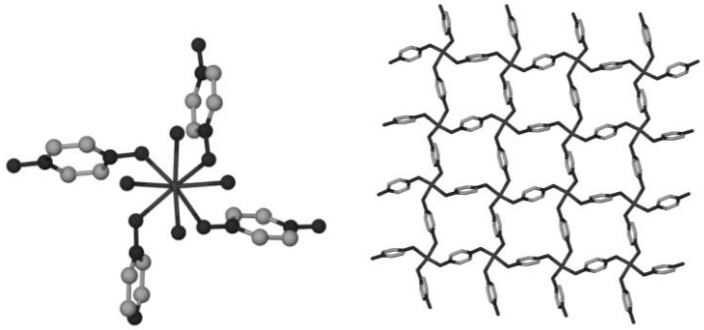

(a) (b)

Figure 7a: The coordination geometry of a single coordinated praseodymium metal center. The chemical formula would be: $[Pr(pzdo)_2(H_2O)_4](CF_3SO_3^-)_3 \bullet 3(H_2O)$
Figure 7b: A network of Pr metal centers interconnected to form a 2-D porous sheet, waters are omitted to reveal the network structure.

With the promising results of the above reactions, it seemed fairly certain that a lanthanide coordination polymer could be synthesized reproducibly and studied in-depth. Earlier in the semester, a set of reactions were prepared using the conditions previously reported, among others, however, none crystallized in time for the completion of this project. Benjamin Quinn-Elmore and I synthesized one coordination network on a number of occasions, which was selected as the focus of this research. With a definitive set of data from the X-Ray Diffractometer, the intermolecular forces for a crystal formed from $Er(CF_3SO_3)_3$ and pyrazine-N,N'-dioxide were studied.

Experimental
(VI)

Synthesis of pyrazine-N,N'-dioxide[xxv]

The organic ligand pyrazine-N,N'-dioxide was prepared using a slightly modified method of Vinciguerra et al.[xxvi] The starting chemical pyrazine (purity ≥99%) was obtained from Sigma Aldrich Chemical Corporation. 4.343 g of pyrazine (purity ≥99%) was combined with 40.0 mL of glacial acetic acid and 20 mL of 35% hydrogen peroxide in a round-bottom flask containing a stir bar. The mixture was heated and stirred at 75ºC on a heating plate under a hood vent. Another 15.1 mL aliquot of 35% hydrogen peroxide was added three hours later and the reaction mixture was heated for an additional 9 hours. After a total of 12 hours in the flask, a 20.0 mL portion of H_2O was added to the mixture and it was distilled at approximately 100ºC to remove the free water. A cloudy yellow oil was derived and removed from the distillation pot. 150 mL of acetone was added to this oil to produce a pure white precipitate. The solution was filtered using a vacuum filtration system and washed twice with hot acetone to remove the un-reacted pyrazine. The damp product (4.308 g) was placed on a watch glass and put under the hood vent to dry overnight. The mass of the dried product was 3.81 g.

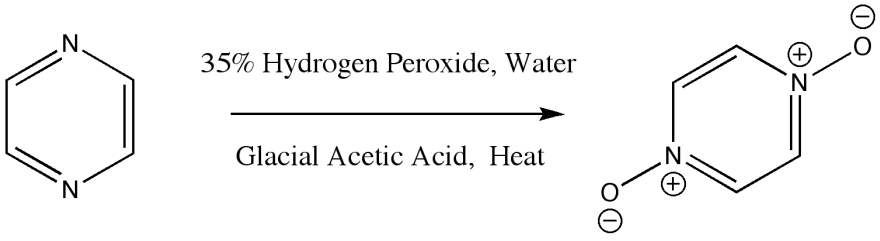

Schematic 1: The abbreviated reaction diagram for conversion of pyrazine (≥99%) to pyrazine-N,N'-dioxide

Dilution of Lanthanide Salt Erbium Triflate[xxvii]

A lanthanide salt in solution was necessary to carry out the layering and combination methods used to form the coordination network. A solution of lanthanide triflate salt was prepared to evaluate the formation process. A 0.0870 M $Er(CF_3SO_3)_3$ solution was prepared by dissolving 0.5455g erbium(III)trifluoromethanesulfonate, 98% by weight, in a volumetric flask using methanol (CH_3OH).

$$(0.5455g)\left(\frac{98g}{100g}\right)x\left(\frac{1mol}{614.47g}\right)x\left(\frac{1}{.010L}\right)=.0870M$$

Synthesis of a coordination polymer between $Er(CF_3SO_3)_3$ and pzdo[xxviii]

(Similar reaction used by BQE on pg 40 of Laboratory Notebook (Allegheny College Chemistry)) Various amounts of $Er(CF_3SO_3)_3$ were used in a series of reactions. A technique called 'layering' was used for these reactions, which allows the two different solutions to gradually mix leading to a slow chemical reaction and eventually crystallization on the test tube walls. The top layer was composed of 0.026g of pyrazine-N,N'-dioxide, 1.5 mL deionized water (H_2O) and 2.5 mL methanol (CH_3OH). The bottom layer consisted of variable amounts of the 0.0870 M $Er(CF_3SO_3)_3$ solution prepared above, 0.754 mL methanol (CH_3OH) and 2.5 mL methylene chloride (CH_2Cl_2) Five volume amounts of the 0.0870 M $Er(CF_3SO_3)_3$ solution were used in five separate reactions, specifically, 1.96 mL, 0.981 mL, 0.492 mL, 0.246 mL, and 0.123 mL.

Both the top and bottom layers were filtered using a sand and fine cotton filled pipette and the top layer was placed above the bottom layer in a 5 mL test tube (Figure 8). The top of the test tube was covered with parafilm to avoid any debris contaminating the solution. A small hole was punctured in the film so that the solvents could slowly

evaporate and lead to gradual crystallization. Three months later, a small pink crystal was found formed on the sidewall of the test tube from the 0.246 mL 0.0870 M $Er(CF_3SO_3)_3$ addition. While other reactions exhibited some evidence of crystallization, upon further study, using XRD, these crystals were merely the ligand precipitating on the test tube walls.

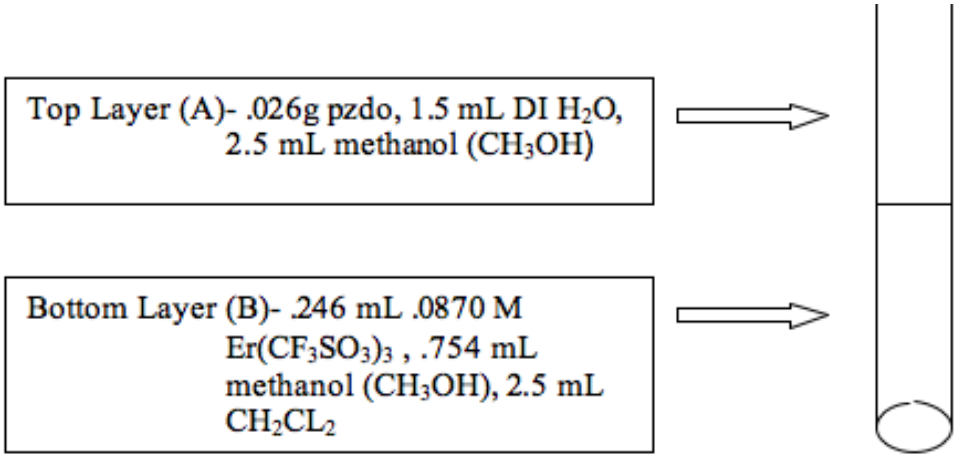

Figure 8: Test tube diagram showing the contents of the Top and Bottom Layers for the crystillization method.

X-Ray Diffraction:

Crystal data for 11_11_13: $C_{13}H_{24}ErF_9N_5O_{21}S_3$, M = 1020.84, pink block, 0.30 × 0.20 × 0.14 mm^3, triclinic, space group P-1 (No. 2), a = 11.2229(16), b = 11.4212(16), c = 13.2263(19) Å, α = 104.325(3), β = 104.679(3), γ = 90.271(3)°, V = 1584.9(4) Å^3, Z = 2, D_c = 2.139 g/cm^3, F_{000} = 1004, Bruker AXS SMART APEX CCD diffractometer, MoKα radiation, λ = 0.71073 Å, T = 100(2)K, $2\theta_{max}$ = 56.6º, 8920 reflections collected, 8920 unique (R_{int} = 0.0000). The structure was solved and refined using the programs SHELXTL 6.14 (Bruker, 2000-2003) and SHELXTL 6.14 respectively. The program X-Seed (Barbour, 1999) was used as an interface to the SHELX programs, and to prepare the figures. Final *GooF* = 1.022, *R1* = 0.0320, *wR2* = 0.0776, *R* indices based on 8325 reflections with I I>2(I) (refinement on F^2), 512 parameters, 14 restraints. Lp and absorption corrections applied, μ = 2.991 mm^{-1}.

The crystal under investigation was found to be non-merohedrally twinned. The orientation matrices for the two components were identified using the program Cell Now, and the two components were integrated using Saint, resulting in a total of 28,195 reflections. 9,641 reflections (5,488 unique ones) involved component 1 only (mean I/sigma = 12.6), 9,364 reflections (5,315 unique ones) involved component 2 only (mean I/sigma = 6.5), and 9,190 reflections (5,420 unique ones) involved both components (mean I/sigma = 13.5). The exact twin matrix identified by the integration program was found to be -1.00102 0.00002 -0.00411, -0.00247 -1.00128 -0.00472, 0.59522 0.56980 1.00325.

The data was corrected for absorption using TWINABS, and the structure was solved using direct methods with only the non-overlapping reflections of component 1.

The structure was refined using the hklf 5 routine with all reflections of component 1 (including the overlapping ones) below a d-spacing threshold of 0.75.

The Rint value given is for all reflections before the cutoff at d = 0.75 and is based on agreement between observed single and composite intensities and those calculated from refined unique intensities and twin fractions (TWINABS (Sheldrick, 2007)).

Results and Discussion
(VII)

Any discussion of the potential applications for lanthanide coordination networks must begin with an in-depth study of the three dimensional structure. Ideally, this structure is a planned engineering result based on targeted properties for the product. In this work we start with a simple objective to reproducibly synthesize a representative coordination polymer. The synthesis of the crystal $[Er(pzdo)_2(H_2O)_4](CF_3SO_3^-)_3 \bullet 3(H_2O) \bullet 1/2(pzdo)$ has been reproducibly synthesized in three separate experiments by two researchers. All reactions yielded identical products as determined by single crystal X-Ray Diffraction methods. The empirical formula produced from the crystal data and structure refinements is Er $C_{13}H_{24}F_9N_5O_{21}S_3$ with the first coordination sphere shown in Figure 9.

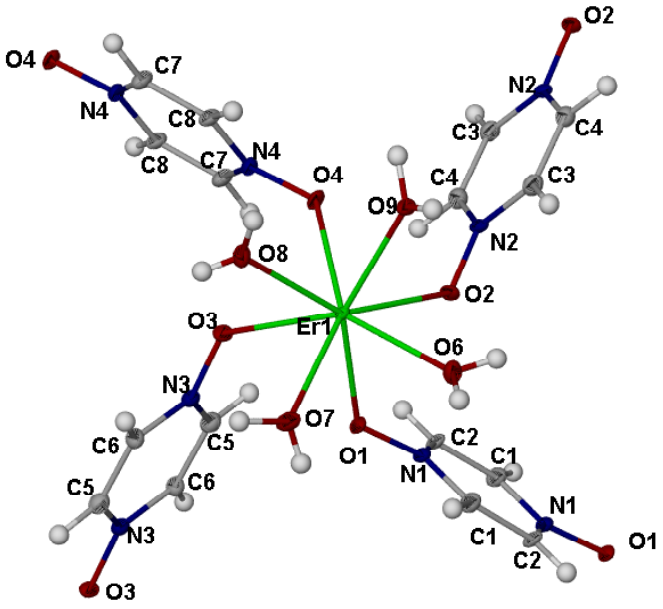

Figure 9: This image shows a single Erbium metal center with coordinated ligands. The exact interactions will be discussed in detail later in the section, however this is a good representation of the primary coordination sphere of the metal center. The metal center Erbium, as well as the bonds between it and the coordinated Oxygen atoms, are green. Oxygen atoms are colored burgundy,

Nitrogen dark blue, and Carbon atoms are colored grey. This figure represents a 50% thermal ellipsoid representation of a single metal center.

In this structure Er is coordinated to 4 pzdo molecules (at O1, O2, O3, and O4) and 4 water molecules (at O6, O7, O8, and O9). The empirical formula obtained from X-Ray Diffraction indicates a stoichiometry of five Nitrogen atoms to each Er^{+3}. Since each pzdo contains two Nitrogen atoms for a total of eight Nitrogens, all of the coordinated pzdo must be bridged pzdo shared by two metal atoms (bidentate), which results in a 4:1 stoichiometry ($N:Er^{+3}$). In order to arrive at a 5:1 ratio, an additional weakly bound pzdo must be shared between adjacent coordination spheres.

A primitive coordination geometry represented in chemical terms in Figure 9 for the primary coordination sphere can also be displayed to show the symmetry elements for the crystal structure for $[Er(pzdo)_2(H_2O)_4](CF_3SO_3^-)_3 \bullet 3(H_2O) \bullet 1/2(pzdo)$. Figures 10 and 11 show these projections from two axes.

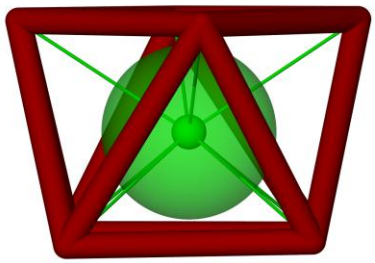

Figure 10: Shows the primitive geometry of the metal center as viewed from the b-axis

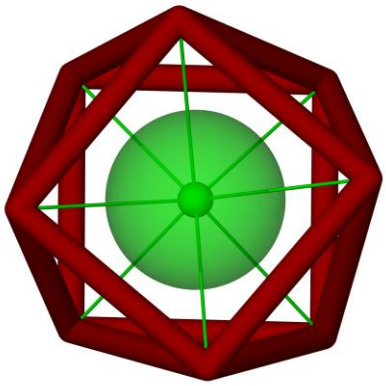

Figure 11: Shows the primitive geometry of the metal center as viewed from the c-axis

Figures 10 and 11 are microscopic with respect to the total crystal system and reflect the geometry within the primary coordination sphere. The eight ligands that surround each Er^{+3} are arranged in two approximate square prismatic configurations that are anti to each other (offset by 45 degrees). This arrangement results in the lowest free energy for the ligand substitution around the central metal ion (lowest repulsive forces).

Working from the empirical formula and considering the atoms incorporated into the primary coordination sphere, the full molecular formula can be derived as [Er $(pzdo)_2(H2O)_4](CF_3SO_3\text{-})_3 \cdot 3(H_2O) \cdot ½(pzdo)$. In addition to the coordinate covalent binding of four pzdo and four water molecules in the primary coordination sphere, each unit has three triflate molecules, three water molecules, and a shared pzdo molecule loosely bound via hydrogen bonding. These weakly bound substituents and their hydrogen bonding relationships are shown in Figure 12.

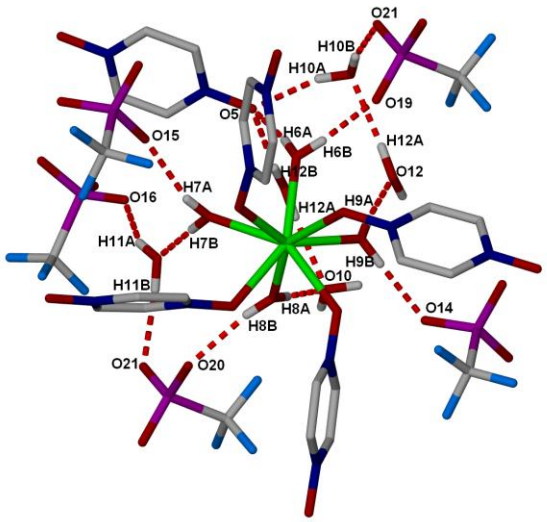

Figure 12: [Er (pzdo)$_2$(H2O)$_4$](CF$_3$SO$_3$-)$_3$ **.** 3(H$_2$O) **.** ½(pzdo). This wireframe figure shows the hydrogen bonding that is present for one metal center. It is the "primary" sphere of coordination as shown in Figures 9, 10, and 11 along with the hydrogen bonded triflate, water, and pzdo molecules. The five $CF_3SO_3^-$ shown are comprised of four shared molecules and one unique to the local metal environment. The seven H_2O molecules shown are comprised of four coordinated and three, which are loosely bound.

When the bidentate pzdo bridges are extended to nearest neighbors, a two dimensional layered structure is formed and shown in Figure 13. The first coordination sphere for this two dimensional structure is shown in Figure 13, and the entire molecular structure including weakly bound substituents in Figure 14. These figures are analogous to Figures 9 & 12 with the bidentate pzdo ligand bridges forming a 2-dimensional network structure. Figure 14 shows the intricacy of the hydrogen bonding that also extends between adjacent metal units.

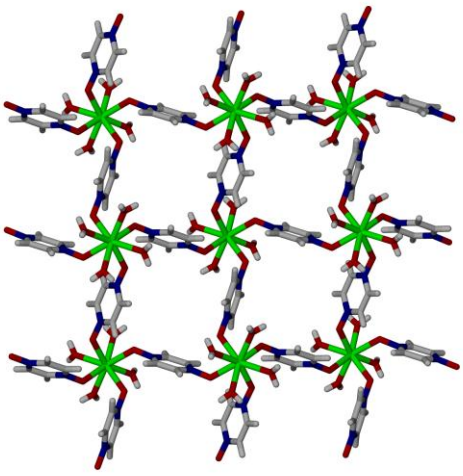

Figure 13: Depicts the 2-D structure looking down the c-axis for [Er $(pzdo)_2(H2O)_4](CF_3SO_3\text{-})_3 \cdot 3(H_2O) \cdot$ ½(pzdo) first coordination sphere.

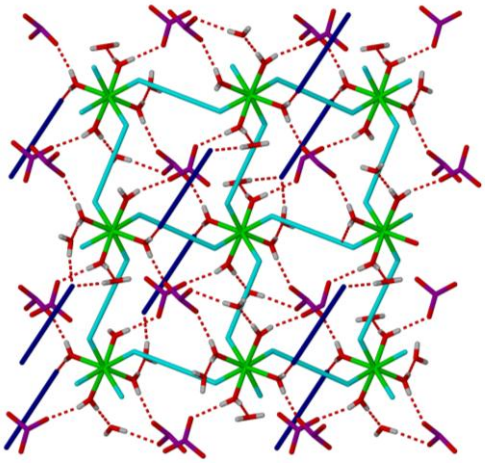

Figure 14: Shows the 2-D view looking down the c-axis for $[Er(pzdo)_2(H2O)_4](CF_3SO_3\text{-})_3 \cdot 3(H_2O) \cdot$ ½(pzdo) including all weakly bound and H-bonded substituents. Water is grey/red, triflate is red/purple, coordinated pzdo is aqua, and non-coordinated pzdo is dark blue. [Color scheme; C-grey, O-red, S-purple]

The layers, as displayed in Figures 13 and 14, are self-assembled as a result of the strong coordinate covalent bonding of the bidentate pzdo ligands to adjacent nearest

neighbor Er^{+3} metal centers and weaker H^{+} bonding forces between triflate, water, and pzdo molecules. These hydrogen bonds are shown in Figure 14 as red dashed lines.

Figure 16 shows 2 of the layers as shown in Figure 15 viewed from the b-axis.

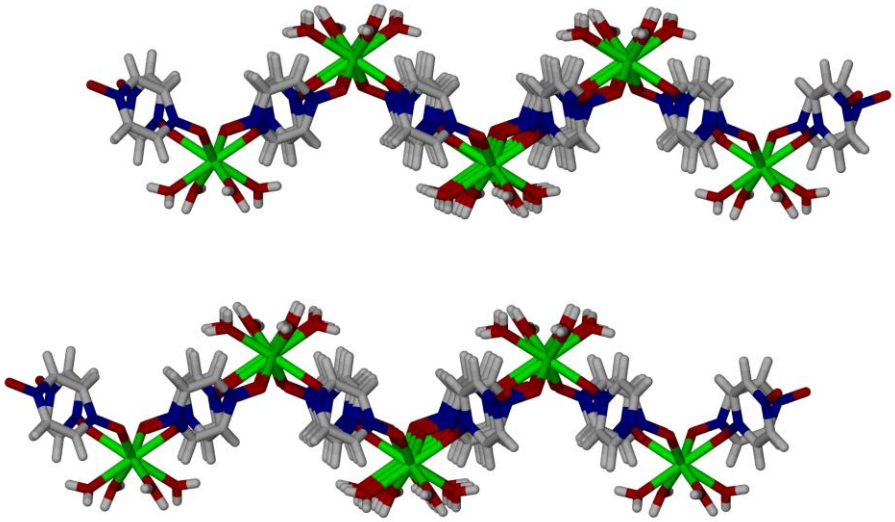

Figure 15: The first coordination sphere for two of the networked layers that bind together to form the 3-D polymer network.

Alternatively this b-axis projection can be generated using a space filled representation rather than the wireframe representations. A space filled representation for the first coordination sphere is shown in Figure 16. Figure 17 shows all substituents, both coordinated and loosely bound, in the space filled representation.

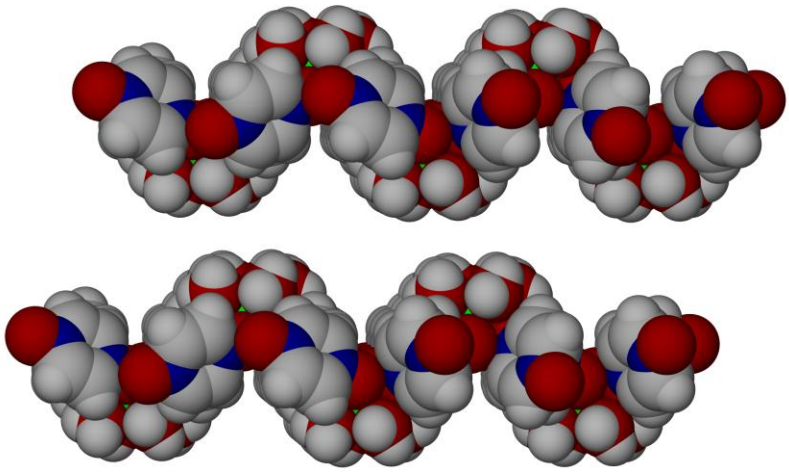

Figure 16: A space filled representation for the first coordination spheres for two networked layers as viewed looking down the b-axis. The grey spheres are C or H depending on size, the red spheres are O from either pdzo or water, and the blue spheres are N from pdzo. The Er^{+3} metal ions are green spheres that are buried in the individual layers at each inflection point.

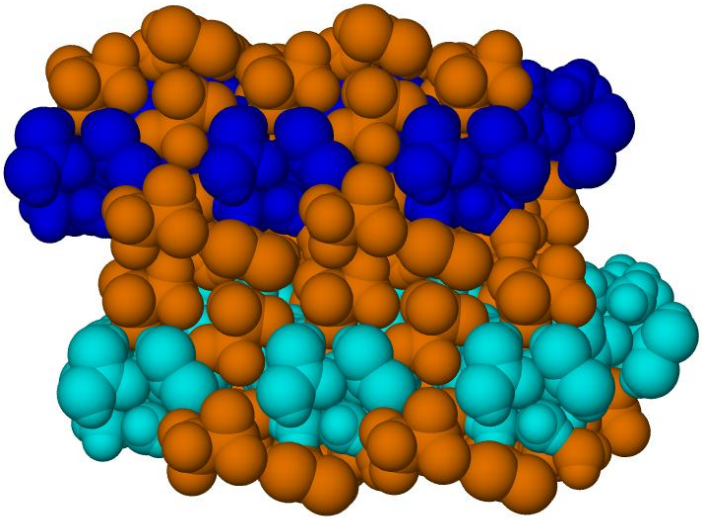

Figure 17: The first coordination space fill diagram shown in Figure 14 is extended to include all weakly bound substituents, which give both the primary coordination networked layers' and the overlapped layers' stable 3-dimensional structure. The aqua and blue spheres represent two networked layers and the

orange spheres represent the weakly bound substituents that cross-link the two layers together.

The same substituents that provide hydrogen bonding within the single layer viewed down the c-axis, as in Figure 14 participate in hydrogen bonding to hold the layers to an ordered structure when viewed in the b-axis. Figure 15 shows two layers down the b-axis in a wireframe representation and includes all non-covalently bound water, pzdo, and triflate molecules and hydrogen bonding that maintains the ordered structure. This format will make it easier to discuss specific bond orientation.

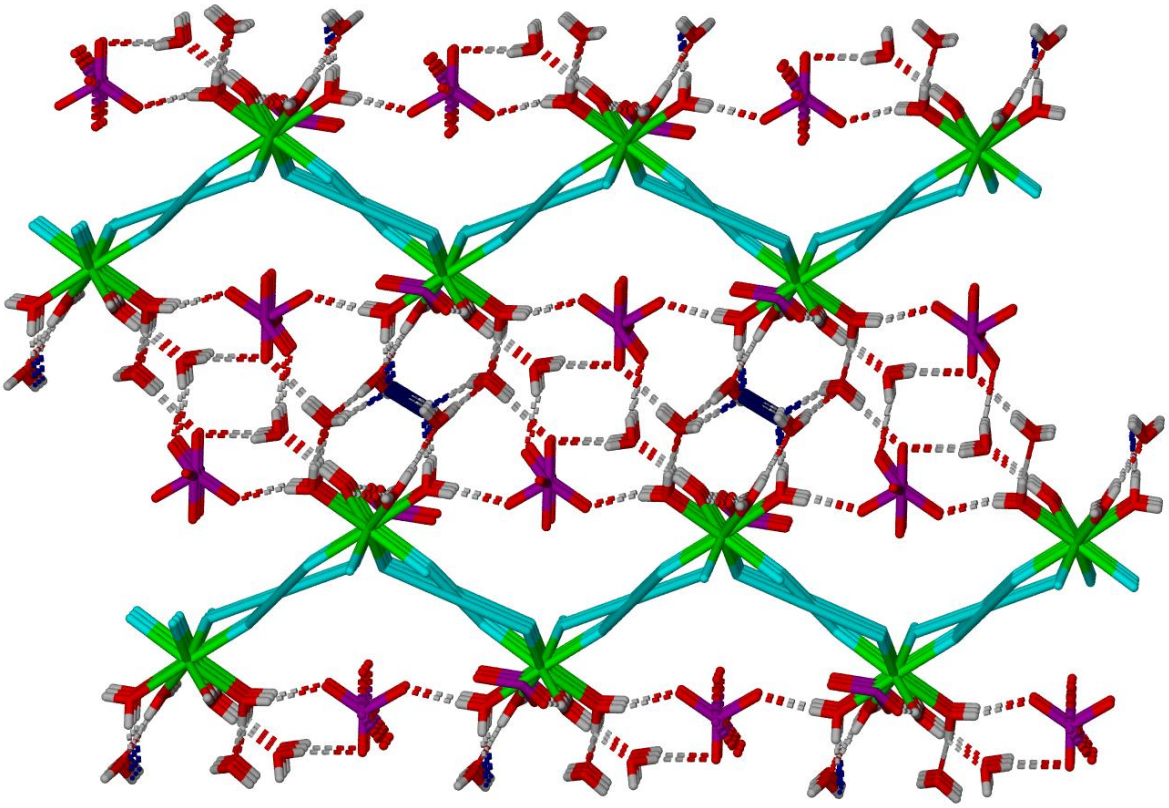

Figure 18: Shows two primary coordination networked layers and the specific hydrogen bonds that bind these two layers together to form a tertiary polymer structure viewed looking down the b-axis. Green bonds are coordinate covalent bonds from the Er^{+3} to each of the eight ligands in the first coordination sphere. Aqua bonds represent the coordinated bidentate pdzo molecules that connect adjacent Er^{+3} atoms. The uncoordinated pdzo molecules can be seen on edge in

dark blue. Water molecules have a red oxygen center and grey hydrogen atoms. Triflate molecules have a purple sulfur center and red ends for the oxygens. The CF_3 of the triflate molecule is not shown for clarity, and all dashed lines represent H-bonding within the network.

Inspection of the interlayer binding reveals the importance of water and triflate anions. Water molecules in the first coordination sphere (coordinate covalent bond with Er^{+3}) bind additionally to the other non-coordinate water molecules as hydrogen bonding donors, triflate sulfate oxygen atoms act as hydrogen bonding acceptors, and uncoordinated pdzo oxygen atoms also act as hydrogen bonding acceptors. Extending from these bound substituents are additional non-coordinated water and triflate molecules in H-bond donor and acceptor roles, which complete the cross-linking between the layers creating the 3-dimensional structure of the crystal. The H-bond donors are water molecules (grey dashes) while the H-bond acceptors are both triflate oxygen atoms and water oxygen atoms (both red dashes) as well as uncoordinated pzdo oxygen atoms (blue dashes). Viewing the system down the a-axis results in a clear appreciation of the ordering of the layers in this crystal system that results from H-bonding forces.

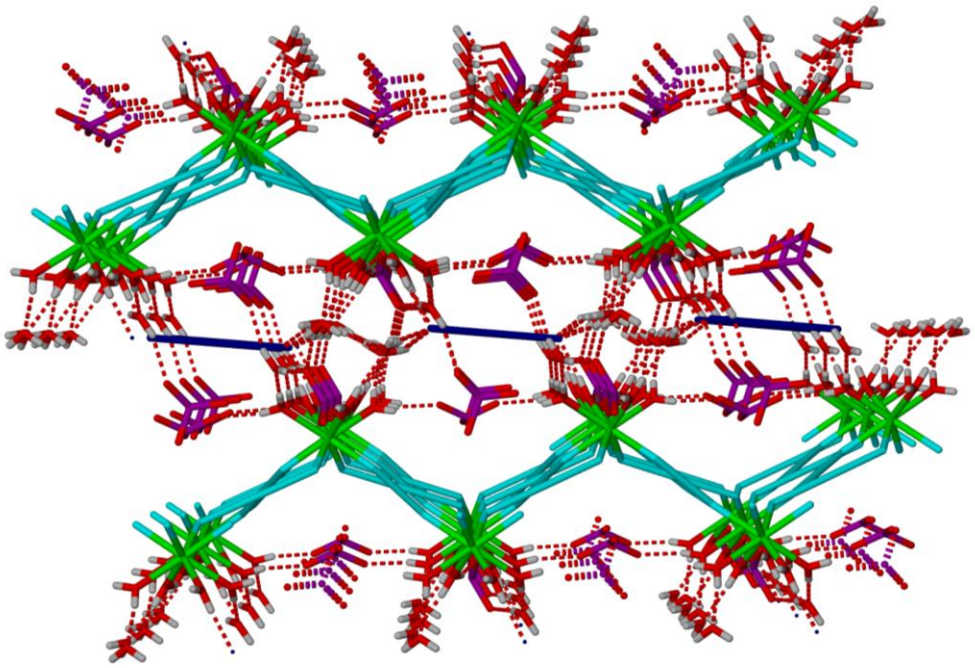

Figure 19: multiple layers of [Er $(pzdo)_2(H2O)_4](CF_3SO_3\text{-})_3 \cdot 3(H_2O) \cdot$ ½(pzdo) viewed down the a-axis and the intricate H-bonding involved.

On a macroscopic level, the crystal system that results from the assembly of these primitive units is morphologically classified as triclinic P-1 by single crystal X-Ray Diffraction analysis. The triclinic crystal system is the least symmetric of the fourteen Bravais lattices that are distributed between the seven crystal systems. In this crystal system, all three angles that describe the crystal are unequal and not equal 90 degrees. In addition, each lattice length vector in each dimension (a, b, and c), are unequal and not mutually orthogonal.

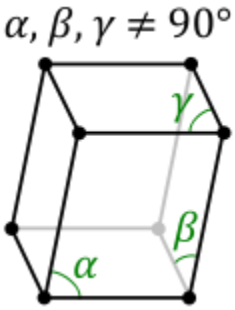

Figure 20: Shows a typical representation for the triclinic crystal system where all angles are not equal to 90 degrees and all lattice vectors are unequal and not orthogonal.

Symmetry considerations in 3-D crystal lattices are complex and best described by group theory. Visualization of multiple axes for reflection, rotation, inversion, and roto-inversion symmetry that can be combined in thirty-two different ways is very difficult. However, it is sufficient to say here that the triclinic crystal systems possess no mirror planes and has only 1-fold symmetry. This is equivalent to having no symmetry at all since the symmetry element is itself.

X-Ray Diffraction results indicate that this triclinic crystal had a "twinned" structure. This phrase, "crystal twinning" means that the two separate crystals share some of the same crystal lattice points in a symmetrical manner. Twinning results in intergrowth and can produce contact or penetration.

Conclusions
(VIII)

Several conclusions can be drawn from this work along with suggestions for future work.

1. A lanthanide coordination polymer was successfully synthesized using the "layering" method and subsequently characterized using X-Ray Diffraction.

2. The methods employed for this work resulted in a time for crystallization of three months, and in other cases longer, if at all. This would appear excessive to facilitate a rapid screening of different systems for selection in particular applications. A suggestion would be to look at reaction conditions, mixing vs. layering, concentrations, temperatures, etc. to determine if these times can be shortened.

3. A series of experiments should be conducted using ligands of different base hardness to probe whether this leads to an acceleration of the time required for crystallation.

4. The $[Er(pzdo)_2(H2O)_4](CF_3SO_3\text{-})_3 \cdot 3(H_2O) \cdot ½(pzdo)$ synthesized here had four water molecules in the primary coordination sphere and three others loosely bound. From Table 3 we see that water is actually a harder base than NO_2^-. The suggested work from (3) could be structured in such a way as to see if the water content of the coordination polymer could be altered through the use of a harder base ligand than pzdo.

5. A high water content may be fine for certain applications, however, for others this may result in a structure that is too hydrophilic in nature. For example, gas adsorption or sequestering may be limited to very polar molecules, and for catalysis the reactions may be limited to more hydrophilic reactants. It is suggested to test this hypothesis with at least one application, to examine the importance of the ligand and loosely bound substituent hydrophilic/hydrophobic character.

Due to the amount of time necessary for this synthesis, it was not possible to examine the viability of other systems. If more time was allotted, or an expedited set of reaction conditions developed, several other tests could have been run to confirm

information about the previously discussed intermolecular forces. An elemental analysis of the crystal could have verified the empirical formula that was given by X-Ray Diffraction. Thermogravimetric Analysis (TGA) could also have been used to test the strength of the loosely coordinated constituents and how they reacted at higher temperatures. While neither of these tests were essential for the study, they would have contributed to the validity of the discussions above.

Previously, in the introduction of this research from last semester, a simple reaction to determine if a network such as this could be used to catalyze an olefin gas was proposed. While time constraints prohibited this from being accomplished, it would have been an interesting experiment to determine if these networks could be used as a catalyst material.

Data Analysis
(IX)

Table 1.

Identification code	07jb009m
Empirical formula	C13 H24 Er F9 N5 O21 S3
Formula weight	1020.84
Temperature	100(2) K
Wavelength	0.71073 A
Crystal system, space group	Triclinic, P-1
Unit cell dimensions	a = 11.2229(16) A alpha = 104.325(3) deg. b = 11.4212(16) A beta = 104.679(3) deg. c = 13.2263(19) A gamma = 90.271(3) deg.
Volume	1584.9(4) A^3
Z, Calculated density	2, 2.139 Mg/m^3
Absorption coefficient	2.991 mm^-1
F(000)	1004
Crystal size	0.30 x 0.20 x 0.14 mm
Theta range for data collection	1.65 to 28.28 deg.
Limiting indices	-14<=h<=14, -15<=k<=14, 0<=l<=17
Reflections collected / unique	8920 / 8920 [R(int) = 0.0000]
Completeness to theta = 28.28	99.1 %
Absorption correction	Semi-empirical from equivalents

Max. and min. transmission	0.658 and 0.286
Refinement method	Full-matrix least-squares on F^2
Data / restraints / parameters	8920 / 14 / 512
Goodness-of-fit on F^2	1.022
Final R indices [I>2sigma(I)]	R1 = 0.0320, wR2 = 0.0776
R indices (all data)	R1 = 0.0346, wR2 = 0.0798
Largest diff. peak and hole	1.995 and -1.546 e.A^-3

Crystal data and Appendix
(X)

Table 2. Atomic coordinates (x 10^4) and equivalent isotropic displacement parameters (A^2 x 10^3) for BQE40D.

U(eq) is defined as one third of the trace of the orthogonalized Uij tensor.

	x	y	z	U(eq)
C(1)	5038(3)	159(3)	6059(3)	13(1)
C(2)	4064(3)	442(3)	4357(3)	15(1)
C(3)	5571(3)	4909(3)	6011(3)	13(1)
C(4)	4100(3)	4135(3)	4346(3)	14(1)
C(5)	634(3)	474(3)	4428(3)	15(1)
C(6)	-66(3)	675(3)	5984(3)	14(1)
C(7)	493(3)	4142(3)	4353(3)	14(1)
C(8)	664(3)	5495(3)	6030(3)	14(1)
C(9)	5960(3)	227(3)	9611(3)	18(1)
C(10)	4274(3)	904(3)	10277(3)	18(1)
C(11)	7340(3)	2287(3)	4243(3)	18(1)
C(12)	-127(4)	1330(3)	1628(3)	20(1)
C(13)	1323(4)	4933(4)	1657(3)	24(1)
Er(1)	3056(1)	3016(1)	6766(1)	10(1)
F(1)	7042(2)	1598(2)	4836(2)	28(1)
F(2)	8518(2)	2125(2)	4237(2)	26(1)
F(3)	7278(2)	3442(2)	4757(2)	22(1)
F(4)	-646(2)	820(2)	2230(2)	33(1)
F(5)	-638(2)	803(2)	602(2)	31(1)
F(6)	-402(2)	2486(2)	1810(2)	30(1)
F(7)	1642(2)	4503(2)	2529(2)	36(1)
F(8)	134(3)	4590(2)	1182(2)	41(1)
F(9)	1982(4)	4430(3)	994(3)	68(1)
N(1)	4111(3)	580(2)	5404(2)	12(1)
N(2)	4677(3)	4052(2)	5355(2)	12(1)
N(3)	559(3)	1146(3)	5413(2)	12(1)

N(4)	1150(3)	4644(3)	5373(2)	13(1)
N(5)	5224(3)	1124(3)	9880(2)	18(1)
O(1)	3190(2)	1074(2)	5779(2)	13(1)
O(2)	4391(2)	3121(2)	5691(2)	13(1)
O(3)	1059(2)	2259(2)	5773(2)	14(1)
O(4)	2269(2)	4329(2)	5712(2)	15(1)
O(5)	5438(3)	2214(2)	9757(2)	23(1)
O(6)	4973(2)	2620(2)	7779(2)	16(1)
O(7)	2649(2)	1725(2)	7809(2)	17(1)
O(8)	1758(2)	4030(2)	7752(2)	17(1)
O(9)	4077(2)	4913(2)	7677(2)	16(1)
O(10)	2612(3)	5912(3)	9489(2)	25(1)
O(11)	1150(3)	1989(3)	9102(2)	29(1)
O(12)	5770(4)	5720(4)	9497(4)	71(2)
O(13)	5118(2)	2111(2)	3023(2)	22(1)
O(14)	6813(2)	2784(2)	2393(2)	19(1)
O(15)	6548(2)	672(2)	2418(2)	20(1)
O(16)	1973(3)	1749(3)	1247(2)	31(1)
O(17)	1751(3)	-18(3)	1925(3)	34(1)
O(18)	1901(2)	1995(2)	3111(2)	17(1)
O(19)	2859(2)	6803(3)	2627(2)	26(1)
O(20)	706(2)	6951(2)	2671(2)	21(1)
O(21)	1271(3)	6895(2)	1007(2)	22(1)
S(1)	6335(1)	1922(1)	2865(1)	15(1)
S(2)	1561(1)	1243(1)	2008(1)	17(1)
S(3)	1576(1)	6581(1)	2031(1)	16(1)

Table 3. Bond lengths [A] and angles [deg] for BQE40D.

C(1)-N(1)	1.348(4)
C(1)-C(2)#1	1.376(5)
C(1)-H(1)	0.9500
C(2)-N(1)	1.342(5)
C(2)-C(1)#1	1.375(5)
C(2)-H(2)	0.9500
C(3)-N(2)	1.359(4)
C(3)-C(4)#2	1.375(5)
C(3)-H(3)	0.9500
C(4)-N(2)	1.354(4)
C(4)-C(3)#2	1.375(5)
C(4)-H(4)	0.9500
C(5)-N(3)	1.362(4)
C(5)-C(6)#3	1.375(5)
C(5)-H(5)	0.9500
C(6)-N(3)	1.347(4)
C(6)-C(5)#3	1.375(5)
C(6)-H(6)	0.9500
C(7)-N(4)	1.342(5)
C(7)-C(8)#4	1.374(5)
C(7)-H(7)	0.9500
C(8)-N(4)	1.351(4)
C(8)-C(7)#4	1.374(5)
C(8)-H(8)	0.9500
C(9)-N(5)	1.355(5)
C(9)-C(10)#5	1.369(5)
C(9)-H(9)	0.9500
C(10)-N(5)	1.350(5)
C(10)-C(9)#5	1.369(5)
C(10)-H(10)	0.9500
C(11)-F(1)	1.335(4)
C(11)-F(3)	1.337(4)
C(11)-F(2)	1.338(4)
C(11)-S(1)	1.830(4)
C(12)-F(5)	1.315(4)
C(12)-F(4)	1.332(4)
C(12)-F(6)	1.334(4)

C(12)-S(2)	1.843(4)
C(13)-F(9)	1.316(5)
C(13)-F(7)	1.331(5)
C(13)-F(8)	1.333(5)
C(13)-S(3)	1.825(4)
Er(1)-O(1)	2.305(2)
Er(1)-O(8)	2.323(2)
Er(1)-O(4)	2.323(2)
Er(1)-O(3)	2.328(2)
Er(1)-O(9)	2.334(3)
Er(1)-O(2)	2.334(2)
Er(1)-O(6)	2.340(3)
Er(1)-O(7)	2.367(3)
N(1)-O(1)	1.326(3)
N(2)-O(2)	1.317(3)
N(3)-O(3)	1.310(4)
N(4)-O(4)	1.306(3)
N(5)-O(5)	1.322(4)
O(6)-H(6A)	0.840(19)
O(6)-H(6B)	0.823(19)
O(7)-H(7A)	0.827(19)
O(7)-H(7B)	0.842(19)
O(8)-H(8A)	0.841(19)
O(8)-H(8B)	0.822(19)
O(9)-H(9A)	0.75(5)
O(9)-H(9B)	0.828(14)
O(10)-H(10A)	0.843(19)
O(10)-H(10B)	0.840(19)
O(11)-H(11A)	0.841(19)
O(11)-H(11B)	0.833(19)
O(12)-H(12A)	0.86(2)
O(12)-H(12B)	0.85(2)
O(13)-S(1)	1.442(3)
O(14)-S(1)	1.455(3)
O(15)-S(1)	1.449(3)
O(16)-S(2)	1.443(3)
O(17)-S(2)	1.439(3)
O(18)-S(2)	1.452(2)
O(19)-S(3)	1.443(3)
O(20)-S(3)	1.448(3)
O(21)-S(3)	1.445(3)

N(1)-C(1)-C(2)#1	119.5(3)

N(1)-C(1)-H(1)	120.2
C(2)#1-C(1)-H(1)	120.2
N(1)-C(2)-C(1)#1	119.5(3)
N(1)-C(2)-H(2)	120.3
C(1)#1-C(2)-H(2)	120.3
N(2)-C(3)-C(4)#2	120.2(3)
N(2)-C(3)-H(3)	119.9
C(4)#2-C(3)-H(3)	119.9
N(2)-C(4)-C(3)#2	119.5(3)
N(2)-C(4)-H(4)	120.3
C(3)#2-C(4)-H(4)	120.3
N(3)-C(5)-C(6)#3	119.9(3)
N(3)-C(5)-H(5)	120.0
C(6)#3-C(5)-H(5)	120.0
N(3)-C(6)-C(5)#3	120.3(3)
N(3)-C(6)-H(6)	119.9
C(5)#3-C(6)-H(6)	119.9
N(4)-C(7)-C(8)#4	120.2(3)
N(4)-C(7)-H(7)	119.9
C(8)#4-C(7)-H(7)	119.9
N(4)-C(8)-C(7)#4	119.9(3)
N(4)-C(8)-H(8)	120.0
C(7)#4-C(8)-H(8)	120.0
N(5)-C(9)-C(10)#5	120.0(3)
N(5)-C(9)-H(9)	120.0
C(10)#5-C(9)-H(9)	120.0
N(5)-C(10)-C(9)#5	120.2(3)
N(5)-C(10)-H(10)	119.9
C(9)#5-C(10)-H(10)	119.9
F(1)-C(11)-F(3)	107.4(3)
F(1)-C(11)-F(2)	107.2(3)
F(3)-C(11)-F(2)	107.7(3)
F(1)-C(11)-S(1)	112.5(3)
F(3)-C(11)-S(1)	111.0(3)
F(2)-C(11)-S(1)	110.9(3)
F(5)-C(12)-F(4)	108.7(3)
F(5)-C(12)-F(6)	107.7(3)
F(4)-C(12)-F(6)	107.1(3)
F(5)-C(12)-S(2)	112.7(3)
F(4)-C(12)-S(2)	110.4(3)
F(6)-C(12)-S(2)	110.0(3)
F(9)-C(13)-F(7)	108.0(3)
F(9)-C(13)-F(8)	108.8(4)

F(7)-C(13)-F(8)	107.5(3)
F(9)-C(13)-S(3)	111.0(3)
F(7)-C(13)-S(3)	110.7(3)
F(8)-C(13)-S(3)	110.7(3)
O(1)-Er(1)-O(8)	137.52(9)
O(1)-Er(1)-O(4)	113.87(8)
O(8)-Er(1)-O(4)	80.27(9)
O(1)-Er(1)-O(3)	72.89(8)
O(8)-Er(1)-O(3)	74.27(9)
O(4)-Er(1)-O(3)	72.46(8)
O(1)-Er(1)-O(9)	146.77(9)
O(8)-Er(1)-O(9)	74.58(9)
O(4)-Er(1)-O(9)	73.55(9)
O(3)-Er(1)-O(9)	136.91(9)
O(1)-Er(1)-O(2)	72.25(8)
O(8)-Er(1)-O(2)	147.21(9)
O(4)-Er(1)-O(2)	72.72(8)
O(3)-Er(1)-O(2)	113.42(8)
O(9)-Er(1)-O(2)	80.14(9)
O(1)-Er(1)-O(6)	80.93(9)
O(8)-Er(1)-O(6)	115.96(9)
O(4)-Er(1)-O(6)	138.25(9)
O(3)-Er(1)-O(6)	147.00(9)
O(9)-Er(1)-O(6)	74.59(9)
O(2)-Er(1)-O(6)	75.85(9)
O(1)-Er(1)-O(7)	74.37(9)
O(8)-Er(1)-O(7)	74.27(9)
O(4)-Er(1)-O(7)	146.91(9)
O(3)-Er(1)-O(7)	80.46(9)
O(9)-Er(1)-O(7)	118.13(9)
O(2)-Er(1)-O(7)	137.32(8)
O(6)-Er(1)-O(7)	73.30(9)
O(1)-N(1)-C(2)	119.1(3)
O(1)-N(1)-C(1)	119.8(3)
C(2)-N(1)-C(1)	121.0(3)
O(2)-N(2)-C(4)	119.8(3)
O(2)-N(2)-C(3)	119.9(3)
C(4)-N(2)-C(3)	120.3(3)
O(3)-N(3)-C(6)	121.0(3)
O(3)-N(3)-C(5)	119.2(3)
C(6)-N(3)-C(5)	119.8(3)
O(4)-N(4)-C(7)	119.6(3)
O(4)-N(4)-C(8)	120.5(3)

C(7)-N(4)-C(8)	119.8(3)
O(5)-N(5)-C(10)	120.1(3)
O(5)-N(5)-C(9)	120.1(3)
C(10)-N(5)-C(9)	119.8(3)
N(1)-O(1)-Er(1)	130.16(19)
N(2)-O(2)-Er(1)	128.32(19)
N(3)-O(3)-Er(1)	130.79(19)
N(4)-O(4)-Er(1)	132.00(19)
Er(1)-O(6)-H(6A)	130(3)
Er(1)-O(6)-H(6B)	122(3)
H(6A)-O(6)-H(6B)	103(4)
Er(1)-O(7)-H(7A)	123(3)
Er(1)-O(7)-H(7B)	130(3)
H(7A)-O(7)-H(7B)	103(4)
Er(1)-O(8)-H(8A)	126(3)
Er(1)-O(8)-H(8B)	124(3)
H(8A)-O(8)-H(8B)	106(4)
Er(1)-O(9)-H(9A)	128(4)
Er(1)-O(9)-H(9B)	124(3)
H(9A)-O(9)-H(9B)	106(5)
H(10A)-O(10)-H(10B)	97(5)
H(11A)-O(11)-H(11B)	107(5)
H(12A)-O(12)-H(12B)	121(7)
O(13)-S(1)-O(15)	114.93(16)
O(13)-S(1)-O(14)	115.57(16)
O(15)-S(1)-O(14)	114.19(16)
O(13)-S(1)-C(11)	103.50(17)
O(15)-S(1)-C(11)	103.81(17)
O(14)-S(1)-C(11)	102.51(17)
O(17)-S(2)-O(16)	115.6(2)
O(17)-S(2)-O(18)	113.66(17)
O(16)-S(2)-O(18)	114.45(18)
O(17)-S(2)-C(12)	105.47(18)
O(16)-S(2)-C(12)	103.83(17)
O(18)-S(2)-C(12)	101.74(16)
O(19)-S(3)-O(21)	115.42(17)
O(19)-S(3)-O(20)	114.99(16)
O(21)-S(3)-O(20)	114.08(17)
O(19)-S(3)-C(13)	103.80(18)
O(21)-S(3)-C(13)	104.02(18)
O(20)-S(3)-C(13)	102.24(17)

Symmetry transformations used to generate equivalent atoms:
#1 -x+1,-y,-z+1 #2 -x+1,-y+1,-z+1
#3 -x,-y,-z+1 #4 -x,-y+1,-z+1 #5 -x+1,-y,-z+2

Table 4. Anisotropic displacement parameters (A^2 x 10^3) for BQE40D.

The anisotropic displacement factor exponent takes the form:
-2 pi^2 [h^2 a*^2 U11 + ... + 2 h k a* b* U12]

	U11	U22	U33	U23	U13	U12
C(1)	14(2)	10(2)	17(2)	4(1)	5(1)	2(1)
C(2)	14(2)	11(2)	20(2)	7(1)	5(1)	4(1)
C(3)	10(2)	14(2)	17(2)	7(1)	6(1)	4(1)
C(4)	12(2)	12(2)	18(2)	3(1)	5(1)	1(1)
C(5)	13(2)	15(2)	17(2)	7(1)	5(1)	4(1)
C(6)	12(2)	13(2)	18(2)	4(1)	6(1)	4(1)
C(7)	13(2)	12(2)	17(2)	4(1)	4(1)	3(1)
C(8)	14(2)	9(2)	19(2)	4(1)	4(1)	4(1)
C(9)	16(2)	25(2)	15(2)	6(2)	5(1)	2(2)
C(10)	16(2)	21(2)	17(2)	3(1)	4(1)	6(1)
C(11)	17(2)	12(2)	24(2)	5(2)	2(2)	1(1)
C(12)	22(2)	17(2)	20(2)	3(2)	6(2)	1(2)
C(13)	27(2)	21(2)	30(2)	9(2)	16(2)	8(2)
Er(1)	9(1)	8(1)	15(1)	3(1)	4(1)	2(1)
F(1)	40(1)	19(1)	22(1)	10(1)	0(1)	-8(1)
F(2)	16(1)	26(1)	35(1)	11(1)	1(1)	6(1)
F(3)	28(1)	11(1)	26(1)	1(1)	7(1)	-1(1)
F(4)	22(1)	46(2)	34(1)	19(1)	5(1)	-7(1)
F(5)	26(1)	40(2)	18(1)	-1(1)	-2(1)	6(1)
F(6)	21(1)	21(1)	44(2)	5(1)	5(1)	9(1)
F(7)	33(1)	30(1)	48(2)	25(1)	2(1)	-2(1)
F(8)	44(2)	24(1)	42(2)	4(1)	-9(1)	-9(1)
F(9)	119(3)	21(1)	99(3)	19(2)	90(3)	28(2)
N(1)	11(1)	7(1)	19(2)	2(1)	6(1)	1(1)
N(2)	13(1)	7(1)	18(2)	6(1)	8(1)	5(1)
N(3)	8(1)	9(1)	18(2)	3(1)	2(1)	1(1)
N(4)	9(1)	11(1)	20(2)	6(1)	4(1)	1(1)
N(5)	19(2)	19(2)	16(2)	6(1)	3(1)	2(1)
O(1)	11(1)	9(1)	21(1)	3(1)	8(1)	4(1)
O(2)	14(1)	8(1)	20(1)	8(1)	6(1)	1(1)

O(3)	10(1)	5(1)	24(1)	1(1)	1(1)	-1(1)
O(4)	9(1)	14(1)	24(1)	9(1)	2(1)	5(1)
O(5)	32(2)	16(1)	21(1)	8(1)	3(1)	0(1)
O(6)	11(1)	18(1)	21(1)	9(1)	3(1)	-1(1)
O(7)	20(1)	14(1)	24(1)	9(1)	12(1)	7(1)
O(8)	14(1)	13(1)	24(1)	1(1)	8(1)	1(1)
O(9)	14(1)	10(1)	22(1)	3(1)	0(1)	0(1)
O(10)	24(2)	20(1)	28(2)	-4(1)	13(1)	-5(1)
O(11)	26(2)	45(2)	26(2)	20(1)	15(1)	18(1)
O(12)	43(2)	73(3)	54(3)	-27(2)	-21(2)	33(2)
O(13)	16(1)	20(1)	30(2)	6(1)	8(1)	6(1)
O(14)	24(1)	15(1)	22(1)	8(1)	6(1)	4(1)
O(15)	23(1)	10(1)	24(1)	2(1)	4(1)	4(1)
O(16)	22(2)	56(2)	21(1)	18(1)	9(1)	10(1)
O(17)	38(2)	17(2)	36(2)	0(1)	-5(1)	13(1)
O(18)	16(1)	16(1)	16(1)	1(1)	4(1)	4(1)
O(19)	13(1)	36(2)	33(2)	19(1)	4(1)	0(1)
O(20)	17(1)	21(1)	25(1)	-1(1)	11(1)	0(1)
O(21)	25(1)	21(1)	22(1)	8(1)	6(1)	8(1)
S(1)	15(1)	11(1)	19(1)	5(1)	4(1)	4(1)
S(2)	18(1)	18(1)	15(1)	3(1)	4(1)	7(1)
S(3)	13(1)	16(1)	19(1)	4(1)	6(1)	4(1)

Table 5. Hydrogen coordinates (x 10^4) and isotropic displacement parameters (A^2 x 10^3) for BQE40D.

	x	y	z	U(eq)
H(1)	5070	276	6802	16
H(2)	3415	757	3907	18
H(3)	5971	4847	6718	15
H(4)	3474	3537	3889	16
H(5)	1080	800	4026	18
H(6)	-113	1140	6674	17
H(7)	828	3534	3894	17
H(8)	1121	5842	6756	17
H(9)	6639	383	9344	22
H(10)	3767	1537	10479	22
H(6A)	5180(40)	2520(40)	8410(20)	24
H(6B)	5620(30)	2870(40)	7700(40)	24
H(7A)	2730(40)	989(19)	7660(40)	25
H(7B)	2180(30)	1800(40)	8220(30)	25
H(8A)	1970(40)	4600(30)	8320(20)	25
H(8B)	1090(30)	3740(40)	7750(40)	25
H(9A)	4580(40)	5080(40)	8190(40)	25
H(9B)	3800(40)	5560(20)	7580(40)	25
H(10A)	3100(40)	6510(30)	9550(40)	37
H(10B)	2200(40)	6280(40)	9900(30)	37
H(11A)	1250(50)	1760(50)	9680(30)	43
H(11B)	480(30)	2310(40)	9010(40)	43
H(12A)	6260(60)	5280(60)	9820(60)	106
H(12B)	5510(70)	6350(50)	9850(60)	106

Table 6. Hydrogen bonds for BQE40D [A and deg.].

D-H...A	d(D-H)	d(H...A)	d(D...A)	<(DHA)
O(6)-H(6A)...O(5)	0.840(19)	1.86(2)	2.692(4)	172(4)
O(6)-H(6B)...O(19)#2	0.823(19)	1.92(2)	2.733(4)	171(5)
O(7)-H(7A)...O(15)#1	0.827(19)	2.05(2)	2.856(4)	163(4)
O(7)-H(7B)...O(11)	0.842(19)	1.81(2)	2.655(4)	179(5)
O(8)-H(8A)...O(10)	0.841(19)	1.85(2)	2.690(4)	172(5)
O(8)-H(8B)...O(20)#4	0.822(19)	2.04(2)	2.844(4)	164(4)
O(9)-H(9A)...O(12)	0.75(5)	1.87(5)	2.612(5)	172(5)
O(9)-H(9B)...O(14)#2	0.828(14)	2.012(16)	2.832(4)	171(4)
O(10)-H(10A)...O(5)#6	0.843(19)	2.06(3)	2.856(4)	158(5)
O(10)-H(10B)...O(21)#7	0.840(19)	2.00(2)	2.826(4)	170(5)
O(11)-H(11A)...O(16)#7	0.841(19)	2.03(3)	2.834(4)	159(5)
O(11)-H(11B)...O(21)#4	0.833(19)	2.17(2)	2.993(4)	171(5)
O(11)-H(11B)...O(20)#4	0.833(19)	2.62(4)	3.203(4)	129(4)
O(12)-H(12A)...O(10)#6	0.86(2)	2.08(2)	2.933(5)	175(8)
O(12)-H(12B)...O(5)#6	0.85(2)	1.99(3)	2.817(5)	163(8)

Symmetry transformations used to generate equivalent atoms:
#1 -x+1,-y,-z+1 #2 -x+1,-y+1,-z+1 #3 -x,-y,-z+1
#4 -x,-y+1,-z+1 #5 -x+1,-y,-z+2 #6 -x+1,-y+1,-z+2
#7 x,y,z+1

References
(XI)

[i] Bowes, C. L.; Qzin, G. A. *Ad*V. *Mater.* **1996**, *8*, 13.

[ii] Xiang, S. C.; Wu, X. T.;Zhang, J. J.; Fu, R. B.; Hu, S. M.; Zhang, X. D. *J. Am. Chem. Soc.* **2005**, *127*, 16352.

[iii] Guillou, N.; Livage, C.; Drillon, M.; Fe´rey, G. *Angew. Chem., Int. Ed.* **2003**, *42*, 5314.

[iv] Knaust, J., *Self-Assembly of One-Two and Three-dimensional coordination networks*., University of Missouri Doctoral Dissertation. **2003.**

[v] Knaust, J., *Self-Assembly of One-Two and Three-dimensional coordination networks*., University of Missouri Doctoral Dissertation. **2003**, 14.

[vi] Huang, You-gui. Wu, Be-lai., Hong, Mao-chun., et al. *Inorg. Chem.*, **2007**, *46* (4), pp 1171–1176.

[vii] Huang, You-gui. Wu, Be-lai., Hong, Mao-chun., et al. *Inorg. Chem.*, **2007**, *46* (4), pp 1174.

[viii] Day, M.C.; Selbin, J., Theoretical Inorganic Chemistry: 2nd Ed., **1962**,pp 120.

[ix] Day, M.C.; Selbin, J., Theoretical Inorganic Chemistry: 2nd Ed., **1962**, pp 401.

[x] Pearson, R.G. *J. Am. Chem. Soc.* **1963**, 85(22), 3533-3539.

[xi] Parr, R.G., Pearson, R.G. *J. Am. Chem. Soc.* **1983**, 105(26) 7512-7516.

[xii] Parr, R.G., Pearson, R.G. *J. Am. Chem. Soc.* **1983**, 105(26) 7512.

[xiii] Lide, D.R. Handbook of Chemistry and Physics: 88th Edition. **2008**, 10-204.

[xiv] Parr, R.G., Pearson, R.G. *J. Am. Chem. Soc.* **1983**, 105(26) 7514.

[xv] Parr, R.G., Pearson, R.G. *J. Am. Chem. Soc.* **1983**, 105(26) 7514.

[xvi] Long, D-L.; Blake, A.J.; Champness, N: Shroder, M. *J.Chem. Soc. Chem. Commun.* **2000,** 1369.

[xvii] Paz, A.; Carlos, R.; Luis, C., *Chem. Mater.*, **2007**, 19, pp 3527-3538.

[xviii] Paz, A.; Carlos, R.; Luis, C., *Chem. Mater.*, **2007**, 19, pp 3531.

[xix] Zhang, Y.F.; Tan, G., *Chinese Chem. Letters.*, **2001**, 13(7), pp 681-682.

[xx] Oliveira, W.; Miotti, R., *J. of Alloys and Comp.*, **2002**, 344, pp 92-95

[xxi] Zocchi, M; Depero, L.E.. *Structural Chemistry*., **1991,** 2 (6), pp 1572-9001.

[xxii] Zocchi, M; Depero, L.E.. *Structural Chemistry*., **1991,** 2 (6), pp 1578.

[xxiii] Shen, T.C.; Ouyang. J.; Wang, F; Hu, C.Y.; Yu, F.; Qian, B; *J. Polymer Sci., Polym. Chem. Ed.*, **1980,** 18, 3345.

[xxiv] Mikheen, N.B. *Inorg. Chim. Acta*, **1984**, 94, 241.

[xxv] Buchner, James Jr. *Laboratory Notebook (Allegheny College Chemistry),* **2006**, pp 1.

[xxvi] Vinciguerra, A., Simpson, P.G.; *Inorg. Chem.* 2 (1963) pp 282.

[xxvii] Buchner, James Jr. *Laboratory Notebook (Allegheny College Chemistry),* **2006**, pp 10.

[xxviii] Buchner, James Jr. *Laboratory Notebook (Allegheny College Chemistry),* **2006**, pp 26-27.